1-1-1974

Cryogenic thin-film electron emitters

Pavel Smejtek
Portland State University

David G. Onn

M. Silver

Citation Details

Smejtek, P., Onn, D., and Silver M., Cryogenic Thin-Film Electron Emitters. Journal of Applied Physics. Vol. 45, no. 1, pp. 119-125. Jan. 1974.

Cryogenic thin-film electron emitters*

David G. Onn†

Department of Physics, University of Delaware, Newark, Delaware 19711

P. Smejtek‡ **and M. Silver**

Department of Physics, University of North Carolina, Chapel Hill, North Carolina 27514
(Received 27 August 1973)

Thin-film electron emitters are described, which operate below 200 °K and below a limiting critical applied voltage (v_c) in a stable temperature-independent regime. Current-voltage characteristics and normal electron energy distributions are presented. Fabrication and operation criteria are outlined. Comparison with temperature-dependent emitters is made, and possible conduction mechanisms discussed briefly.

INTRODUCTION

Since their first operation by Mead[1] thin-film electron emitters, often referred to as cold-cathode emitters, have been the subject of many investigations.[2-10] A review of thin-film emitter research has been given by Crowell and Sze,[11] and contains further references and a summary of the physical basis of their operation. These emitters have not received wide-spread application because of their short lifetime and instability at room temperature. However, we have, for some time, used them at temperatures below 200 °K during studies of electron states in cryogenic fluids.[12-16]

At cryogenic temperatures we find that thin-film emitters provide a reliable, stable, and long-lasting source of currents up to 30 nA in vacuum. The electron emission that we use is associated with a temperature-independent conduction mechanism which can be identified clearly only if the emitter is operated, from the very beginning, at cryogenic temperatures. A temperature-dependent conduction mechanism, with associated unstable emission, can be developed by operating the emitters at temperatures above about 200 °K or by exceeding a critical internal field strength within the insulating layer. The latter mechanism appears to be the one most widely studied by the majority of previous investigators.

The normal energy distributions, at cryogenic temperatures, of the electrons emitted in the low-current temperature-independent mode differ markedly from the distributions previously observed from these emitters at higher temperatures. The distribution is almost completely independent of the emitter driving voltage and insulator thickness for a wide range of both parameters, while the temperature-dependent emission, once generated, has an energy distribution with properties very similar to those described by previous investigators.

As long as the emitters are retained in the temperature-independent emitting mode we observe no emission (down to 10^{-14} A) at energies less than the work function of the metal emitting surface, whereas once this mode has been disturbed, as discussed below, emission is observed below the work-function energy level. Despite operation in the temperature-independent mode for very long periods of time, there is no sign of destruction of the emitting surface, whereas operation above the critical voltage and temperature leads ultimately to the surface disruption and destruction often reported.[4,7,9]

A typical emitter at cryogenic temperatures provides a maximum emission current i_e of about 10 nA from an area of 0.1 cm^2 with a dc applied voltage v_d between 7 and 15 V, depending on insulator thickness. The device conduction current i_d through the insulator does not exceed about 15 μA under these conditions, nor at any time during stable operation. The currents mentioned above are in marked contrast to the emission currents of microamps and device currents of milliamps often reported in earlier studies at room temperature and 77 °K. We can only achieve such high emission and conduction currents by operating emitters in the self-destructive unstable mode associated with temperature-dependent emission and conduction currents. The temperature-independent mode in which we operate emitters seems to have been overlooked previously because the motivation for much of the research was to produce a high-current device for technological application at room temperature. We find that, provided the emitters are operated *first and only* at cryogenic temperatures, they provide a constant stable current in a dc mode for many hours at 77 °K, and almost indefinitely at 4.2 °K. The normal energy distributions indicate that the average emitted electron energy is then about 1 eV.

PHYSICAL BASIS OF OPERATION

The simplified schematic of the energy levels involved in the operation of a thin-film emitter is shown

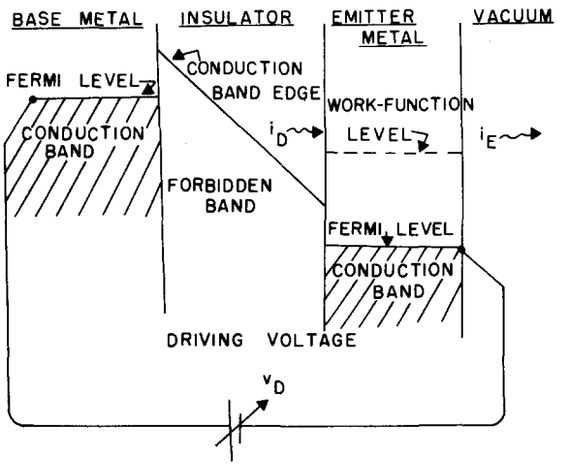

FIG. 1. Schematic energy-band diagram of thin-film electron emitter.

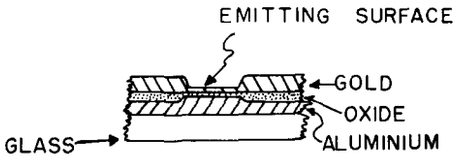

FIG. 2. Cross section of thin-film emitter.

in Fig. 1. A base metal layer (aluminum) is covered with an oxide layer, generally more than 70 Å thick, which in turn is covered with a metal layer (gold) about 100 Å thick. A voltage greater than that of the work function of gold is applied between the metal layers. Electrons are conducted through the oxide layer into the gold. Some retain enough energy to escape from the gold surface since electron-electron scattering, the main loss mechanism in the gold layer, has a mean free path comparable to the thickness of the gold layer. [11]

Several conduction mechanisms within the oxide layer are possible, including direct tunneling into the oxide conduction band, thermal excitation into the conduction band, and tunneling through impurity states, filaments, and other defect states in the oxide layer. Direct metal-metal tunneling is not probable at these insulator thicknesses, generally being observed when insulating layers are less than 50 Å thin. These mechanisms have been discussed by various investigators. [1-9,11] We note that extended study of these emitters at 4.2 °K has not previously been carried out, and only limited studies at 77 °K exist. After describing the construction, operation, and characteristics of our devices at these cryogenic temperatures, we will briefly discuss the conduction mechanisms that appear to be effective.

EMITTER FABRICATION

We have found that the procedure described below gives the most consistent results for devices to be operated in the cryogenic temperature range. The cross section of one successful design is shown in Fig. 2. Other arrangements of the films are possible, but a common feature of successful designs we have used is that they limit emission of electrons to a small window of thin oxide covered by thin noble metal and are designed to prevent spurious emission from sharp or unmasked edges. Since we use wet electrolysis to produce the oxide layer, the emitters could not be maintained under vacuum at all times, but simple cleaning procedures between construction phases gave rise to a 90% success rate.

As substrates we used polished optical-grade glass, 2.5×3.5 cm, large enough to hold three parallel emitters. The substrates were initially washed in a sequence of mild detergent, hot distilled water, cold ethyl alcohol, and hot isopropyl alcohol. From the hot isopropyl alcohol the substrate was rapidly transferred to a bell-jar evaporator, which was evacuated before the substrate had a chance to cool. Discharge cleaning was carried out using a 300-V ac discharge in nitrogen gas at about 100 μ pressure. The bell jar was then oil-diffusion pumped to about 2×10^{-8} Torr, where the base aluminum layer was evaporated to a thickness of about 1500—2000 Å.

Electrolysis was carried out in a dilute solution of tartaric acid, titrated to a pH of 5.5 with ammonium hydroxide. This treatment yields an oxide thickness of 13 Å per electrolyzing volt. [17,18] We created oxide layers from 65 to about 300 Å. During electrolysis the voltage is reversed in order to perfect the oxide layer. [19] Very low electrolysis currents were used, 30 min being needed to create a 100-Å-thick oxide layer as the voltage was increased in small steps. Edge breakdowns were reduced by electrolyzing the aluminum outside the emitting window by an extra 25%. After each electrolysis the wash cycle was repeated to remove every trace of electrolyte from the emitter surface.

After the final washing, the oxidized layer was returned, still hot, to the evaporator mask for deposition of the gold emission surface. The thickness of the gold in the emitting window was monitored as being 100 Å, though usually the electrical resistance of the layer was used to determine the deposition end point. Thick contact tabs to the window were evaporated first. The completed emitters could be stored for several weeks at room temperature in a desiccator, without deterioration, but did not survive as long in the normal laboratory atmosphere.

CRITERIA FOR STABLE EMISSION

As a result of making and testing several hundred emitters, we have established that there are several stringent criteria that must be observed if the stable emission, available at low temperatures, is to be obtained. These criteria appear to be more important to consistent success than precautions taken during fabrication. The most important is that the emitters should never be operated, or even tested, above a critical maximum temperature T_c which is about 200 °K. In practice, all of our emitters are cooled and first operated at 77 or 160 °K. Hickmott[4] and others had noted the existence of a critical temperature close to 200 °K below which voltage-controlled negative resistance (VCNR) established by room-temperature operation disappeared. Our emitters, by virtue of precooling, have not had VCNR established and do not immediately display it when warmed unless, during their cryogenic operation, a second criterion for stable operation is violated.

The second criterion is that a critical maximum voltage v_c determined quite precisely by study of the "aging" process discussed below should not be exceeded. If this voltage is exceeded, even below T_c, then unstable emission that is temperature dependent is initiated, and on warming, VCNR appears at once. We will outline procedures used in establishing the value of v_c and discuss the significance of v_c before discussing more general properties of the emitters, including their electron energy distributions.

The aging of thin-film emitters has been reported several times. [7,20,21] The emission current i_e and the conduction current i_d decay with time when a constant voltage v_d is applied. Conversely, the resistance of the device increases with time. We find the aging process

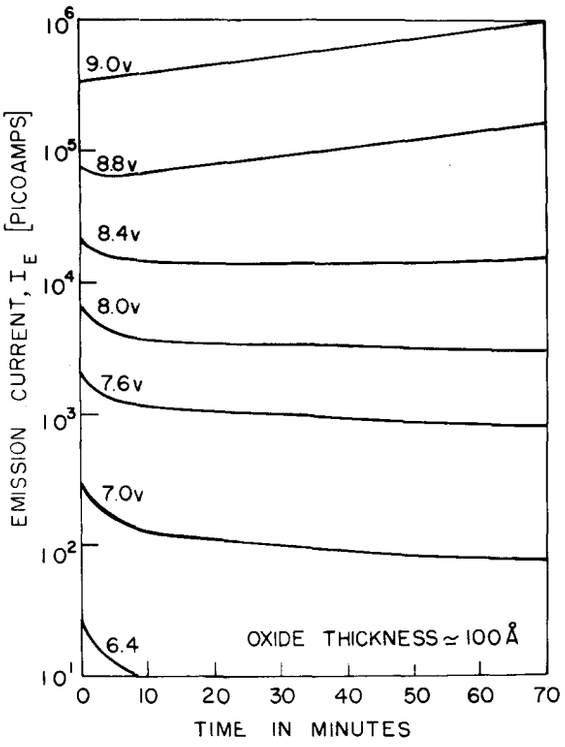

FIG. 3. Emission current as a function of time for various applied voltages.

is essential in determining v_c. First, it is important that the anticipated v_c not be applied immediately, even at temperatures below T_c. Rather, the emitter must be aged in a series of small steps approaching v_c for a few minutes at each step.

The emission current obtained in such a step sequence is shown as a function of time in Fig. 3. At values of v_d (the applied voltage) up to 8 V the emission current i_e decays with time, whereas from 8.4 V upwards an initial decay is followed by a current increase that ultimately leads to destruction of the device. By 9.0 V no decay is observed and destruction starts at once. Though periods of stable emission do occur at voltages from 8.4 V upwards, they are short. Generally i_e ultimately becomes unstable and the device lifetime is limited.

For the emitter properties shown 8 V would be the best operating voltage for highest stable emission and long-term operation. The data shown was obtained at 4.2 °K, but v_c, for a given oxide thickness, has the same value within ±0.5 V up to about 200 °K. The value of v_c increases with increasing oxide thickness, almost proportionately, though with considerable scatter. Since there are three emitters per substrate, we often sacrifice one in order to determine v_c precisely for the remaining pair.

The existence of v_c as a critical voltage suggests that a second conduction mechanism, associated with the less-stable emission, is initiated in the oxide layer once v_d has exceeded v_c. Furthermore, evidence for this is obtained from the changes in the current-voltage characteristics (i_e vs v_d and i_d vs v_d) that occur once v_c is exceeded, even at temperatures less than T_c. In Fig. 4 i_e is plotted against $1/v_d$ for a device with $v_c = 8.2$ V. The emitters were aged at the voltages shown as v_a. As long as $v_d < v_c$ the characteristics, were shown as solid lines having steep slopes which could be obtained and repeated. Once the emitter had operated with $v_d > v_c$, the characteristics shown as dashed lines, having a less-steep slope, were obtained. The change in slope represents an increase in emission current which is voltage dependent and is most significant at low voltages. Emission was also obtained for v_d less than the work function of gold once v_c had been exceeded.

Reducing v_d below v_c does not return the characteristics to their earlier shape, obtained for $v_d < v_c$, suggesting that the new emission is the result of a new conduction process. However, if v_d is reversed for a few seconds the old characteristics with steep slopes are obtained again for $v_d < v_c$ in the forward direction. The restoration is generally only temporary, and rapid reversion to the characteristics typical of $v_d > v_c$ occurs, along with the return of instability in emission and emission under the work function. As we discuss below, the original electron energy distribution is *not* regenerated after reversal.

The characteristics obtained for $v_d < v_c$ are temperature independent up to about 200 °K, whereas those obtained after v_c is exceeded are temperature dependent, showing increasing conduction and emission with increasing temperature, and seeming to develop above 200 °K into the conduction and emission associated with

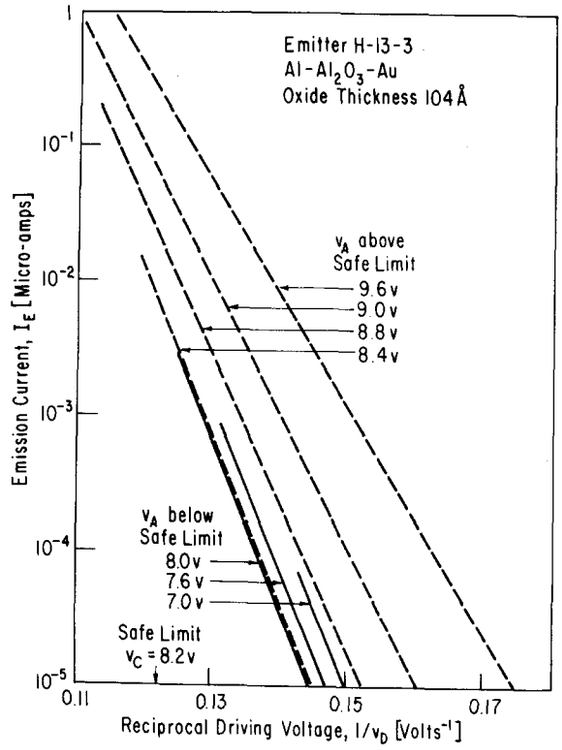

FIG. 4. i_e vs $1/v_d$ for an emitter aged in steps to the voltage limits v_A.

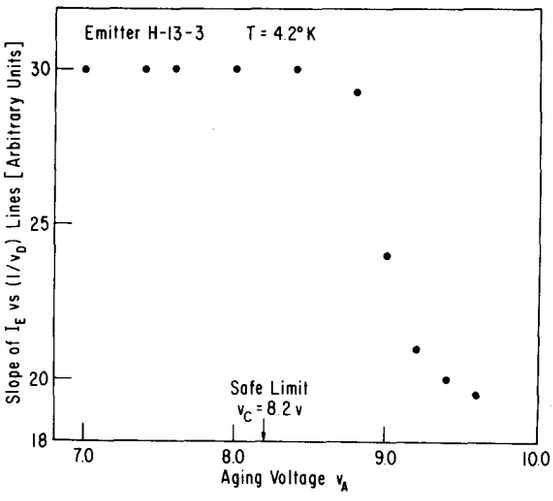

FIG. 5. Slope of the characteristics of Fig. 4 showing the rapid change at the critical voltage.

VCNR.[4] We have not yet studied this temperature dependence in detail.

In Fig. 5 we plot the slope of the emission characteristics from Fig. 4 as a function of v_d. The marked transition in slope is clearly seen at about 8.2 V, corresponding closely to the value of v_c obtained by studying the time variation of i_e as shown in Fig. 3 for a similar emitter.

Similar changes occur in the i_d-vs-v_d characteristics once v_c is exceeded, though we have not studied these in such detail. As long as v_d has not exceeded v_c, then at 4.2 °K for voltages up to 3 V the conduction current in the oxide layer, i_d, is typically less than 100 pA, whereas once v_c has been exceeded i_d may exceed 100 nA at 3 V. This change is only partially removed by reversal of v_d. As the temperature is increased this anomalous current, which is also temperature dependent, becomes the VCNR peak observed by Hickmott and others, and may exceed 30 mA at 3 V and 300 °K.

For reference we show in Fig. 6 a typical set of current-voltage characteristics obtained with an emitter operating stably at 4.2 °K after careful "aging" below its critical voltage v_c. The graph of i_e vs $1/v_d$ is almost exactly a straight line for four decades in i_e, though it should be noted that the range of v_d is so limited (7.6–9.8 V) that a plot of i_e vs $1/v_d^2$ is also almost exactly a straight line. This fact points up the difficulty of interpreting such current-voltage characteristics in terms of internal conduction mechanisms, particularly when the added factor of metal-oxide contact potentials is brought in to reinterpret v_d in terms of an internal field in the oxide.

The conduction current i_d is also shown in Fig. 6. The changing slope of this characteristic is a reflection of the increasing efficiency i_e/i_d as the critical voltage is approached. We have not obtained efficiencies of greater than 5×10^{-4} as long as our emitters operated in the stable mode, below v_c and T_c. The properties of emitters with silver and aluminum emitting surfaces have characteristics similar to those described for the gold-surfaced emitters, except that they were generally less efficient.

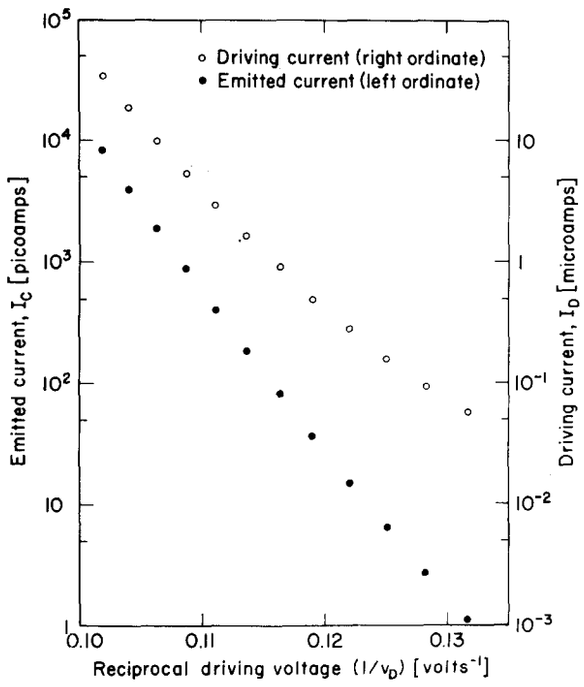

FIG. 6. Typical set of current-voltage characteristics for a stable emitter.

NORMAL ENERGY DISTRIBUTIONS

The normal energy distributions of the emitted electrons were studied, using a modulated grid spectrometer shown schematically in Fig. 7. A planar grid system was used, limiting studies to the normal energy distribution. More complete studies are planned using a spherical grid system. The present results are valuable as a comparison with other published normal energy distributions for similar emitters, generally at higher temperatures.[2,3,5] The entire spectrometer grid system of Fig. 7 could be cooled to 4.2 °K.

Grid g_1 is maintained at a positive potential, large enough to prevent electron loss to fringe fields between the aluminum and gold surfaces of the emitter.[3] The g_1

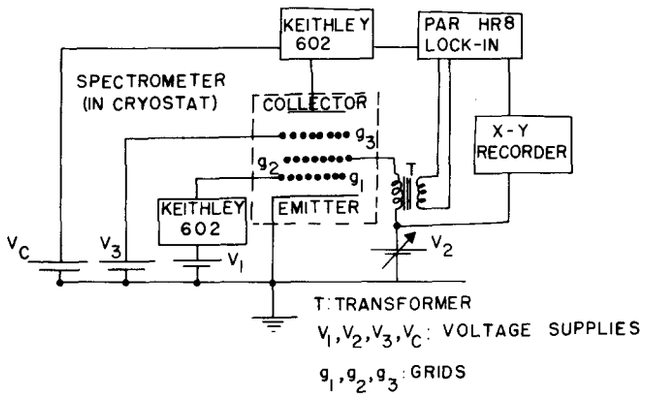

FIG. 7. Circuit used for normal energy distributions.

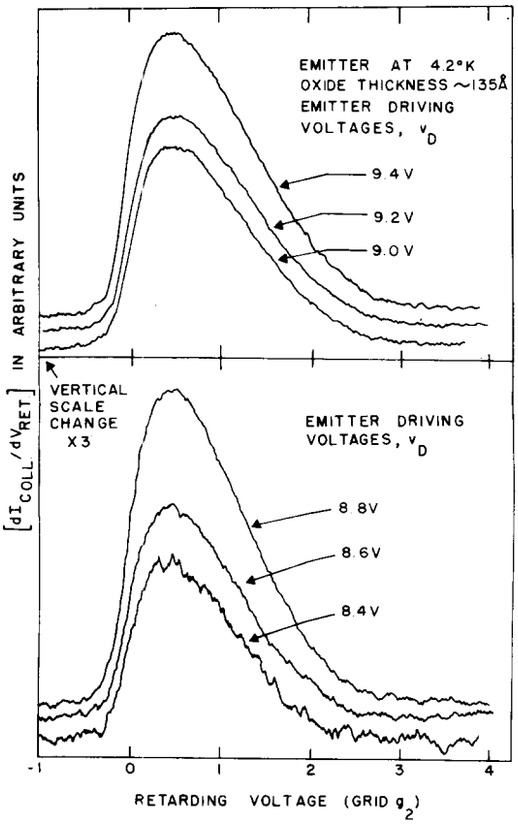

FIG. 8. Normal energy distributions for a stable emitter for voltages from 8.4 to 9.4 V.

grid current is monitored by a Keithley model 602 electrometer and is typically less than 5% of the total emission current. This, and the remaining grids, are gold mesh, 500 lines/in. Grid g_2 can be both swept in voltage by the source V_2 (driven by a small motor) and modulated by the reference output from the PAR HR8 lock-in amplifier. Modulation signals as low as 50-mV peak to peak were used. Grid g_3 is maintained slightly negative in relation to the collector to prevent backscattering of electrons from the collector. The collector current is monitored by a second Keithley 602 electrometer operating off-ground. The dc current is read directly, while the ac component is detected by the lock-in amplifier and displayed on the recorder. By sweeping V_2, the normal energy distribution is obtained directly on the X-Y recorder, while if the lock-in is detecting the second harmonic the slope of the normal energy distribution is obtained. This ac method of obtaining energy distribution is more direct and gives better resolution than the retarding dc collector system used by most previous investigators. We carried out a comparison with the dc retarding method in our own system and found that if carefully applied it provides a reasonable picture of the energy distribution characteristics, such as peak position and width at half-height, so that we feel justified in making comparisons between our ac method and the results obtained by others on dc systems.

The modulated grid system provides an excellent monitor of unstable emission from the devices. Such emission causes extreme noise levels and only a considerable increase in the lock-in time constant and a reduced sweep rate permit approximate energy distributions to be obtained. This was a constant source of difficulty when operation of emitters above v_c was being studied.

A set of normal energy distributions obtained with the spectrometer operating at 4.2 °K is shown in Fig. 8. The critical voltage v_c for this emitter was 9.8 V and was not exceeded at any time. The oxide thickness was about 130 Å. Distributions were obtained with the operating voltage v_d varying from 8.4 to 9.4 V, the emitter being aged to a constant emission current at each value of v_d as described earlier. The emission current increased by one and a half orders of magnitude between the lowest and highest voltage traces.

The normal energy distribution is almost independent of v_d, despite the increased emission current. The width at half-height (WHH) of the distribution increases only from 1.4 to 1.5 V, and the width at quarter height increases only slightly more, from 1.9 to 2.1 V, while the operating voltage has increased by 1 V. A shift in the maximum is not detectable. Thus, an emitter, properly aged and operated, is an electron source of variable current strength, but almost constant energy distribution. Results at 77 °K are similar, and the energy distributions are no wider than at 4.2 °K.

This result is quite different from that of Kanter and Fiebelman[2,5] who, operating an emitter at room temperature, found that the energy distribution WHH was linearly dependent on v_d. They found WHH greater than 4 V for an emitter with parameters closest to the one used for Fig. 8. Furthermore, our emission current was stable at all times, whereas they mention instabilities particularly at high values of v_d. Their peak emission currents were, however, as high 1 μA, whereas ours were less than 20 nA.

We also studied the dependence of energy distribution structure on oxide thickness, since the results shown in Fig. 8 suggest that this may be the only way to obtain a variety of energy distributions. Our emitters were aged and operated close to but not exceeding v_c and had oxide thicknesses ranging from 70 to 160 Å. Operation was at 4.2 and 77 °K, and no temperature effects were seen. We did observe some increase in WHH of the distributions as we used increasing oxide thickness, from 0.8 V for the thinnest to 1.3 V for the thickest oxide. Distribution maxima were all at 0.5 ± 0.2 V with no detectable dependence on oxide thickness. Results on oxide layers thicker than 160 Å were inconclusive.

The increase in WHH observed by Kanter as discussed by Handy[5] is consistently greater than ours, except for the thinnest oxide layers. Furthermore, Kanter's peak energy position is observed to increase linearly with oxide thickness, though again we note the different operating regimes of our emitters and those of Kanter.

Once the critical voltage v_c for stable temperature-independent emitter operation had been exceeded, irreversible chances in the energy distribution took place. Although, as we noted early, the low-voltage current-voltage characteristics can be repeated by reversing v_d

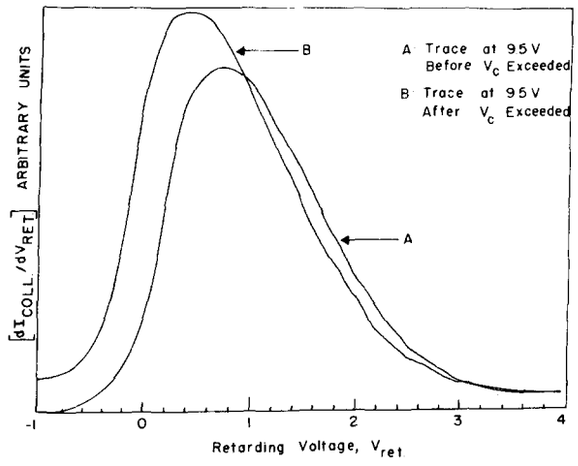

FIG. 9. Change in normal energy distribution before and after v_c is exceeded. Both curves taken at same v_d.

(see discussion of Figs. 4 and 4), we could find no way of returning to the original energy distributions once v_c had been exceeded.

The change in distribution is shown in Fig. 9. This emitter was operated at 9.5 V to obtain trace A, before being operated at 12 V, exceeding the critical voltage of 9.8 V. Returning to 9.5 V produced the broader distribution shown as trace B, containing a considerable increase in the number of lower-energy electrons. Use of lower value of v_d produced a similar broad distribution. Once operating in this regime (i.e., with v_d having once exceeded v_c) the energy distributions and current characteristics became temperature dependent and dependent on v_d. In addition, VCNR was observed at higher temperatures, and the dependence of the WHH, peak position, etc., of the energy distribution agreed quite well with the observations of Kanter and others.

SUMMARY DISCUSSION

We have identified a regime in which thin-film electron emitters can be operated as reliable stable current sources at cryogenic temperatures. Provided that the procedures we describe are adhered to, i.e., operating voltage is kept below the critical value v_c and temperature is below 200 °K. Emission-current—voltage characteristics similar to those in Fig. 5 can be expected, together with normal energy distributions similar to those in Fig. 8. These characteristics and distributions are virtually unchanged up to about 200 °K and appear to be associated with a temperature-independent conduction mechanism through the oxide layer.

On the other hand, once either v_c is exceeded or ope-operation is carried out above 200 °K the temperature-independent conduction and emission are either replaced or masked by a temperature-dependent conduction and emission with properties similar to those observed by other investigators. Detailed analysis of conduction mechanisms in thin oxide layers through analysis of the current-voltage characteristics is known to be uncertain due to the limited range of applied voltage (see discussion of Fig. 6) and the added factor of assuming appropriate contact potentials at the metal-oxide interfaces in order to obtain true internal fields in the oxide layer. Analysis of electron energy distributions is also difficult, since the observed emission is only a small fraction of the energy distribution in the oxide layer. Consequently, we will not here undertake complete analysis of our characteristics and energy distributions here. We do note, however, that conduction mechanisms associated with impurity-band conduction,[22,23] filamentary growth,[24] and internal temperature-field emission and related processes[5,7,8,11,25,26] are all temperature dependent, whereas direct tunneling processes are largely temperature independent.[11,12]

We provisionally conclude, therefore, that the cryogenic regime of operation in the stable temperature-independent mode is the result of tunneling into the oxide conduction band under the high-field conditions prevailing in the oxide layer. Direct metal-metal tunneling is not probable at these insulator thicknesses. The current-voltage characteristics and electron energy distributions that we present here are the first that we know of associated with this temperature-independent conduction mechanism.

At higher temperatures, or when v_c has once been exceeded, the characteristics and energy distributions are similar enough to those of other investigators that mechanisms proposed or discussed by them are probably effective.

Whatever may finally be concluded as to the appropriate operating mechanism of these devices, our main interest was in developing them to a reliable state for operation as electron sources at cryogenic temperatures. We feel that with appropriate care and precautions as described above they can be made and operated quite straightforwardly and will find much wider application than at present.

*Supported in part by the Army Research Office, Durham, the National Science Foundation, and the Materials Research Center of the University of North Carolina under contract No. SD-100 from the Advanced Research Projects Agency.
†Supported in part by NSF Grant No. GH-37278 to the University of Delaware.
‡Present address: Department of Physics, Portland State University, Portland, Ore. 97207.
[1]C.A. Mead, J. Appl. Phys. 32, 646 (1961).
[2]H. Kanter and W.A. Feibelman, J. Appl. Phys. 33, 12 (1962).
[3]R.E. Collins and L.N. Davies, Solid-State Electron. 7, 445 (1964).
[4]T.W. Hickmott, J. Appl. Phys. 36, 1885 (1965).
[5]R.M. Handy, J. Appl. Phys. 37, 4620 (1066).
[6]R.R. Verderber and J.G. Simmons, Radio Electron. Eng. 33, 347 (1967).
[7]E.D. Savoye and D.E. Anderson, J. Appl. Phys. 38, 3245 (1967).
[8]H. Kanter, Appl. Phys. Lett. 12, 243 (1968).
[9]H. Ahmed, J. Appl. Phys. 43, 242 (1972).
[10]D.G. Onn, P. Smejtek, and M. Silver, Proceedings of the

XIIIth International Conference on Low-Temperature Physics, Boulder, Colo., 1972 (unpublished).
[11]C.R. Crowell and S.M. Sze, in *Physics of Thin Films* (Academic, New York, 1967), Vol. 4, p.350ff.
[12]D.G. Onn and M. Silver, Phys. Rev. **183**, 295 (1969).
[13]D.G. Onn and M. Silver, Phys. Rev. A **3**, 1773 (1971).
[14]P. Smejtek, M. Silver, K.S. Dy, and D.G. Onn, J. Chem. Phys. **59**, 1374 (1973).
[15]J.A. Jahnke and M. Silver, Rev. Sci. Instrum. **44**, 776 (1973).
[16]J.A. Jahnke and M. Silver, Chem. Phys. Lett. **19**, 231 (1973).
[17]G. Hass, J. Opt. Soc. Am. **19**, 532 (1949).
[18]L. Young, *Anodic Oxide Films* (Academic, New York, 1961).
[19]C.L. Standley and L.I. Maissel, J. Appl. Phys. **35**, 1530 (1964).
[20]R.M. Handy, Phys. Rev. **126**, 1968 (1962).
[21]J.G. Simmons, Phys. Rev. Lett. **10**, 10 (1963).
[22]L.A. Harris, J. Appl. Phys. **35**, 268 (1964).
[23]J.G. Simmons and R.R. Verderber, Proc. Roy. Soc. A **301**, 77 (1967).
[24]G. Dearnaley, Phys. Lett. A **25**, 760 (1967).
[25]P.R. Emtage and W. Tantraporn, Phys. Rev. Lett. **8**, 267 (1962).
[26]S.R. Pollack, J. Appl. Phys. **34**, 877 (1963).